Supporting Information

Molecular packing structure of fibrin fibers resolved by X-ray scattering and molecular modeling: Supplementary Information

Karin A. Jansen[#], Artem Zhmurov[#], Bart E. Vos, Giuseppe Portale, Daniel H. Merino, Rustem I. Litvinov, Valerie Tutwiler, Nicholas A. Kurniawan, Wim Bras, John W. Weisel, Valeri Barsegov[*], and Gijsje H. Koenderink [*]

[#]K.A. Jansen and A. Zhmurov contributed equally to this work
***Corresponding authors:** g.h.koenderink@tudelft.nl, Valeri_Barsegov@uml.edu

Supplementary methods: analysis of turbidimetry data

We fit turbidimetry data to obtain the number of protofibrils, N_p, and the mass-length ratio, ν, for each fibrin gel condition studied using a method previously proposed by Ferri et al [1]. For the reader's convenience, we have included a flow chart of the fitting procedure (Figure S1), where we refer to the specific equations from the work of Ferri et al. Briefly, the model approximates the fibers as solid cylinders and takes into account the fractal structure of the branched network in terms of the network fractal dimension D_m. We furthermore include a correction for the wavelength dispersion of the solvent refractive index $n_s(\lambda)$ and the differential refractive index $dn(\lambda)/dc$ (with c the protein mass concentration) based on Cauchy's empirical relations[28]:

$$n_s(\lambda) = A_1 + A_2/\lambda^2 \quad \text{(S1)}$$

$$dn/dc(\lambda) = B_1 + B_2/\lambda^2 \quad \text{(S2)}$$

with optical constants A_1 = 1.3270, A_2 = 3.0595·10^{-3} μm^2, B_1 = 0.1856 cm^3/g and B_2 = 2.550·10^{-3} cm^{3}μm^2/g from Refs.[28, 43]. The model involves the two structural parameters characteristic of the fibers that we aim to determine, namely their radius R and mass-length ratio ν, and two parameters characterizing the network structure, namely its fractal dimension D_m and mesh size ξ. The turbidity data are fitted to the model with R and ν as floating parameters and D_m and ξ as input parameters. Values for D_m were determined for each network by Fourier transforming the confocal reflection microscopy images, radially integrating the Fourier transformed images to calculate a power spectrum, and fitting the power spectrum to a power-law $I(q) \propto q^{-D_m}$ over a range of spatial frequencies q corresponding to length scales between 0.6 μm (three times the diffraction limit) and 10 μm (1/10th of the image size).[9-30, 60] Resulting values for D_m varied between 1.4 and 1.5. The network mesh size ξ and the fiber mass-length ratio ν are interrelated:

$$\xi = (c/\nu)^{-1/2} = (c/\nu_{pf}N_p)^{-1/2}, \quad \text{(S3)}$$

where ν_{pf} = 1.55·10^{11} Da/cm is the mass-length ratio of the fibrin protofibril[44]. We therefore used an iterative fitting procedure to find the best-fit values for ξ, ν and R for each individual sample (Fig. S1). We first performed a fit to the wavelength-dependent turbidity data using an initial

guess for ξ taken from a visual inspection of the confocal data. This first fit gave a best-fit value for ν. Next, we repeated the fitting procedure with ξ updated from the ν-value obtained from the preceding fit using Equation (S3) until ξ and ν changed by less than <1%. Convergence typically required fewer than 5 iterations. Example fits are shown in Figure S2 of the ESI. From the best-fit values of R and ν, we calculated the fiber mass density $\rho = \nu/\pi R^2$. The outcomes of the analysis for all the fibrin conditions studied in the paper are collected in Supporting Table 1 of the ESI.

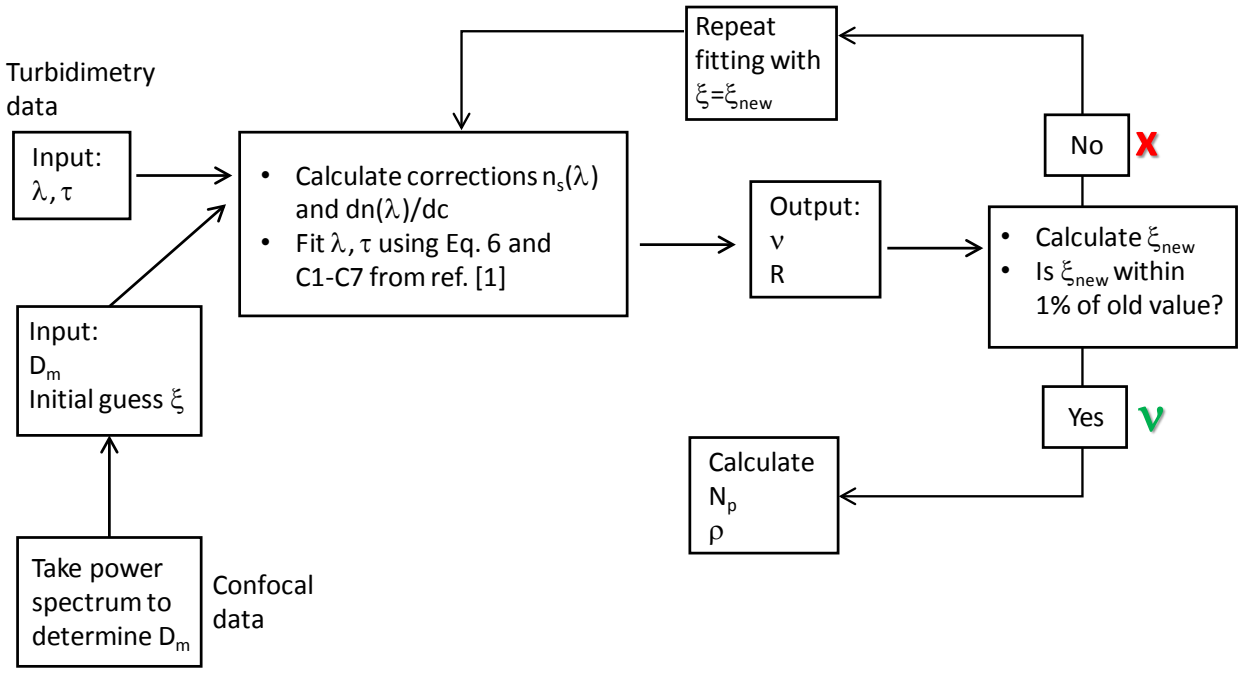

Figure S1. Flow diagram for the determination of the fiber bundle size N_p (or equivalently the mass-length ratio ν) and its radius R from the turbidity data. First, an input value for the network fractal dimension D_m was obtained by Fourier analysis of confocal images, and an initial guess for the mesh size was made by visual inspection of the confocal images (initial guess ξ). The solvent refractive index $n_s(\lambda)$ and differential refractive index $dn(\lambda)/dc$ were calculated using Equations S1 and S2 in the Supplementary Methods section. Next, wavelength-dependent turbidity data were fitted using equation 6 from the main text of ref. [1]. From these fits, we obtained the fiber radius and its mass-length ratio. Using equation S3, we then calculate the new mesh size ξ_{new} from the obtained best-fit value for ν. If this value is within 1% of the old value, we report the number of protofibrils and the density of the fibrin fibers, N_p and ρ, respectively. Otherwise, the fitting procedure is repeated using the new mesh size value.

Supporting Table: turbidimetry data

Nr.	Fibrin(ogen) concentration and condition details	R (nm)	N_p [1]	fiber density [mg/ml], ρ	mesh size (μm), ξ	mass/length ($\cdot 10^{13}$ Da/cm), ν	D_m
(1)	8 mg/ml, prepared in fine clot conditions	7.5 – 15	2.0 ± 1.3	71.2 – 285	-	0.03 ± 0.02	-
(2)	8 mg/ml, prepared from as-received stock	134 ± 87	47 ± 0.5	11.6 ± 8.9	0.49 ± 0.43	0.45 ± 0.14	1.4
(3a)	4 mg/ml, prepared from dialyzed stock	127 ± 20	291 ± 37	148 ± 13	2.66 ± 0.30	4.5 ± 1.0	1.4
(3b)	8 mg/ml, prepared from dialyzed stock	136 ± 5.6	435 ± 107	196± 60.4	1.16 ± 0.15	6.6 ± 1.6	1.4
(4)	4 mg/ml, prepared from gel-filtered stock	109 ± 16	368 ± 52	255 ± 13	1.51 ± 0.19	5.6 ± 1.4	1.5

Table S1. Structural characterization of the different fibrin networks used in this study. Numbers correspond to the assembly conditions as numbered in the Materials and Methods section. The fiber thickness N_p and protein mass density ρ for coarse (thick fiber) networks prepared according to conditions (2), (3) and (4) were determined by fitting the wavelength dependence of the turbidity to a theoretical model for thick fibers [1]. The data are reported as averages ± error of the mean based on at least 3 repeats per condition. For fine (thin-fiber) networks prepared according to condition (1), the wavelength-dependent turbidity was fitted to the Carr model for thin fibers [2] to determine ν (average ± error of the mean based on 3 repeats). For the fiber radius, we quote an approximate range, taken from an earlier study of our lab [3] where we imaged fine networks by transmission electron microscopy. The corresponding fiber density range should be regarded as indicative only given the polydispersity in *R* and the assumption of a uniform cylindrical fiber.

References

1. Ferri, F., et al., *Size and Density of Fibers in Fibrin and Other Filamentous Networks from Turbidimetry: Beyond a Revisited Carr–Hermans Method, Accounting for Fractality and Porosity.* Macromolecules, 2015. **48**(15): p. 5423-5432.
2. Carr, M. and J. Hermans, *Size and density of fibrin fibers from turbidity.* Macromolecules, 1978. **11**: p. 46-50.
3. Piechocka, I.K., et al., *Multi-scale strain-stiffening of semiflexible bundle networks.* Soft Matter, 2016. **12**(7): p. 2145-56.

Additional supporting figures

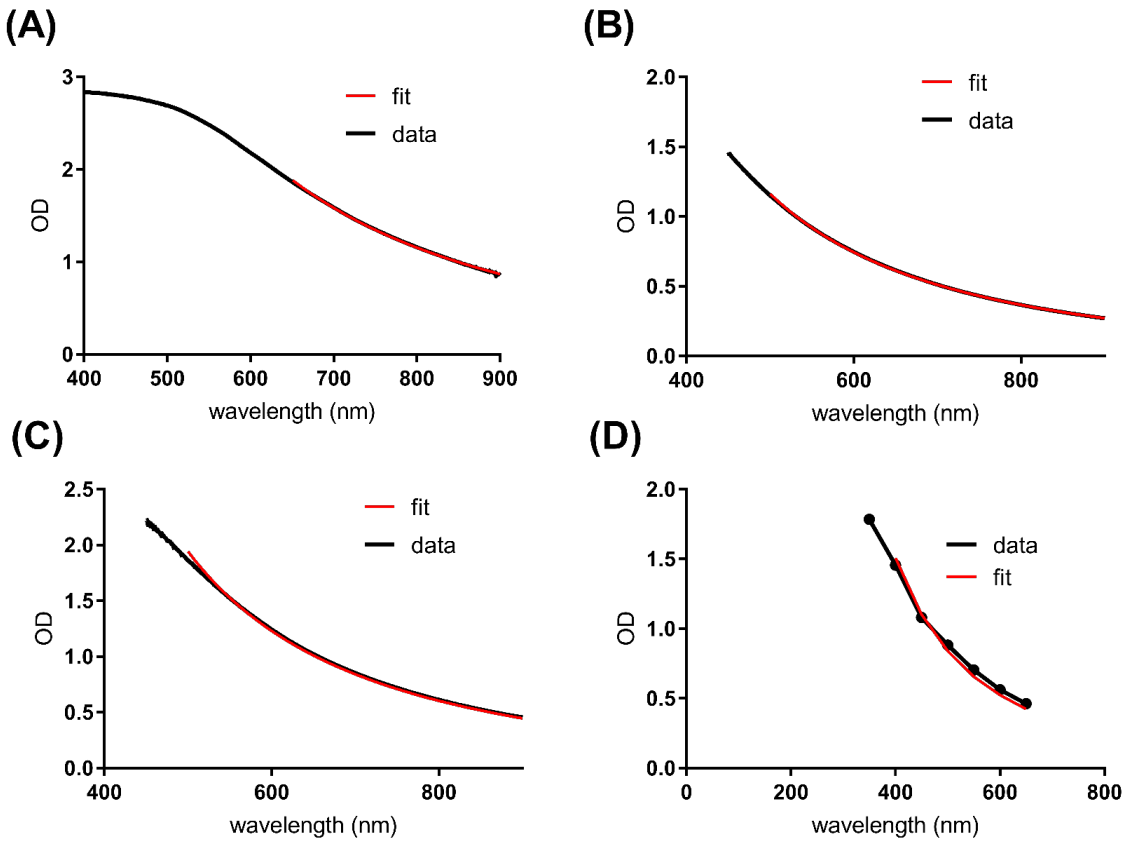

Figure S2. Examples of wavelength-dependent turbidity measurements (black lines) on various fibrin networks together with fits (red lines) to a theoretical model for light scattering from isotropic fibrous networks (see Supplementary Methods section and Supplementary Figure S1 for details). The fit results are summarized in Supporting Table 1. (A) Fibrin network prepared from dialysed fibrinogen stock (3 mg/mL). (B) Network prepared from gel-filtered fibrinogen stock (4 mg/ml). (C) Network prepared from dialysed fibrinogen stock (8 mg/ml). (D) Network prepared from as-received fibrinogen stock (8 mg/ml).

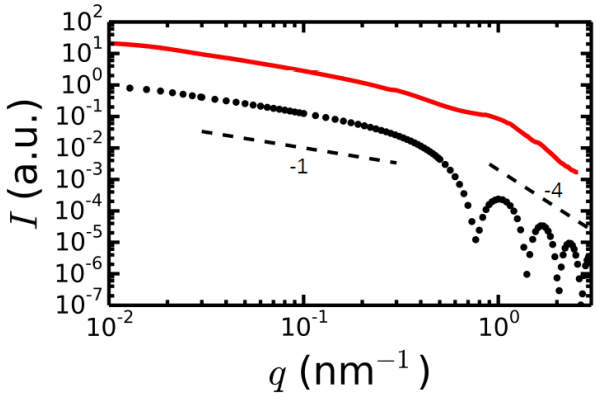

Figure S3. The calculated form factor of a cylinder (black circles) having the dimensions of a fibrin protofibril of 5 fibrin subunits in length (subunit length of 46 nm) and a diameter of 10 nm, compared with the theoretical SAXS profile of fibrin protofibrils reconstructed based on the full-atom structure of oligomer FO6-5 (red line). Curves are shifted along the y-axis for clarity. The dashed lines indicate power laws with exponents of -1 (Guinier regime) and -4 (Porod regime), respectively.

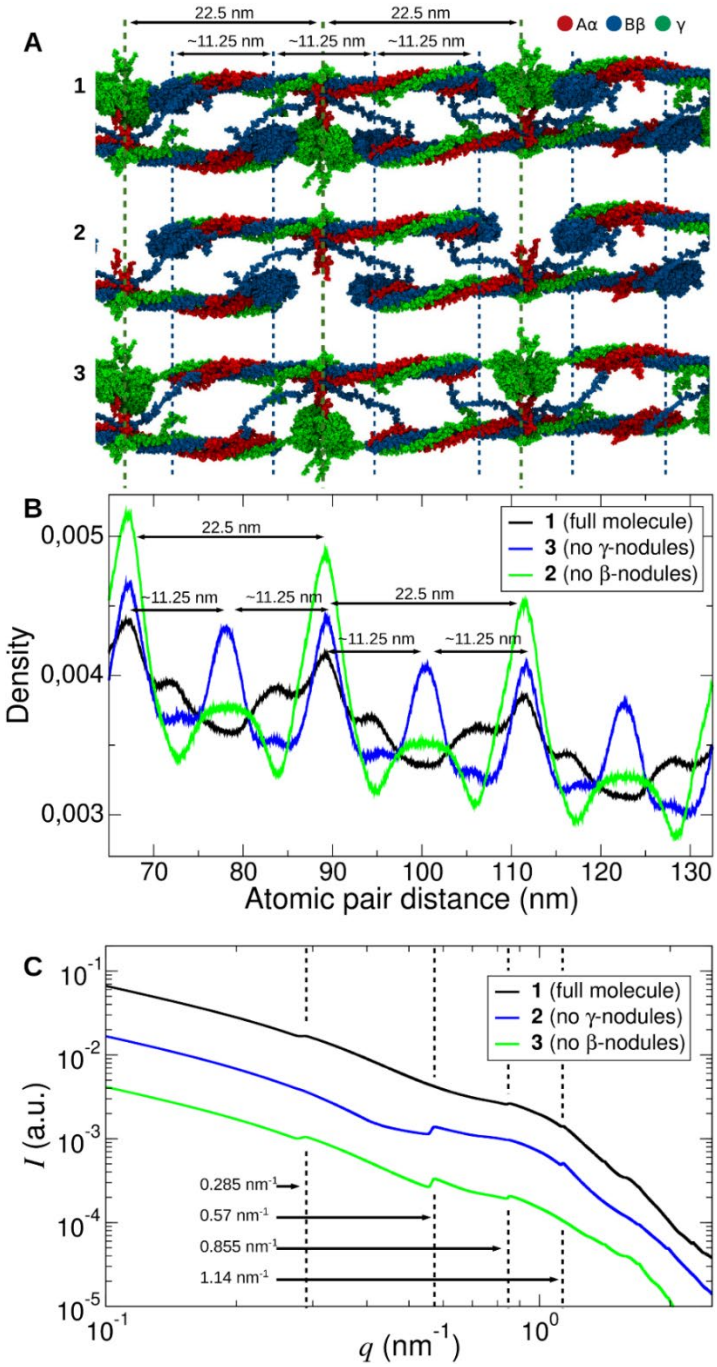

Figure S4: (A) Structures of the two-stranded intact fibrin protofibril (**1**), and protofibril fragments obtained by the removal of the γ-nodules (**2**) and the β-nodules (**3**). Vertical lines show the main 22.5-nm periodicity of the structure and the secondary 11.25-nm periodicity due to the specific orientation of the β-nodules. (B) The distribution of atomic pair distances between 65 and 130 nm for the structures 1-3 shown in panel A. (C) The scattering profiles *I* vs. *q* corresponding to the distributions of atomic pair distances for structures 1-3 from panel B.

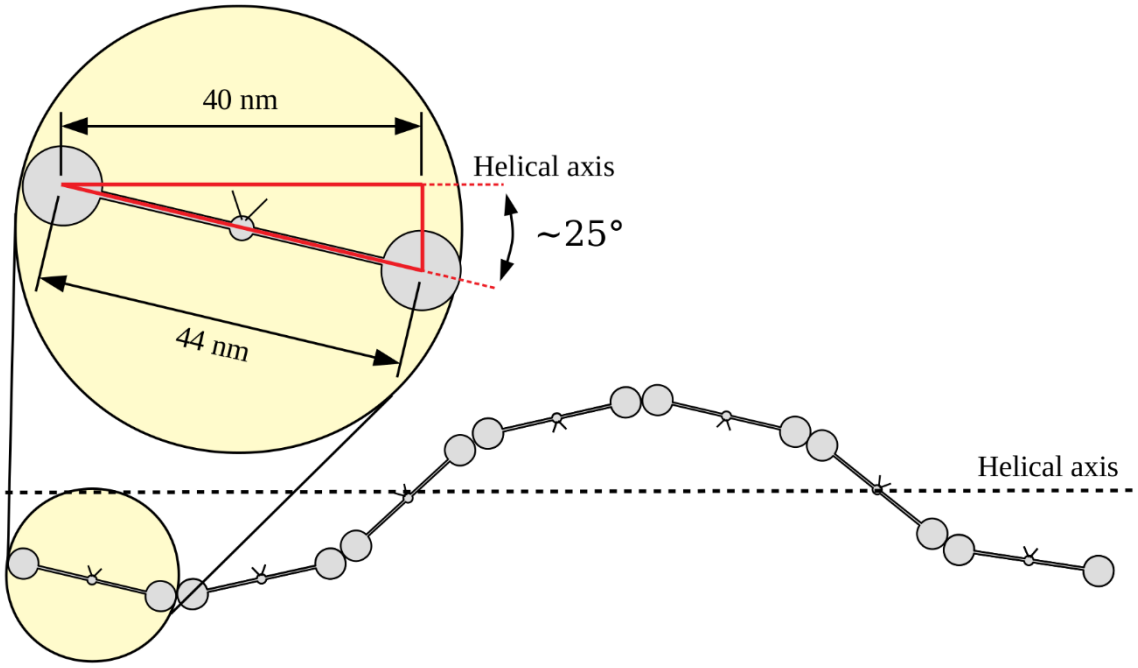

Figure S5. Schematic of a single stranded fibrin oligomer, highlighting the helical twist inside a fibrin bundle. Due to the helical structure of fibrin oligomers, the average distance between the centers-of-mass of the two globular ends of the molecule projected along the helical axis is 40 nm.

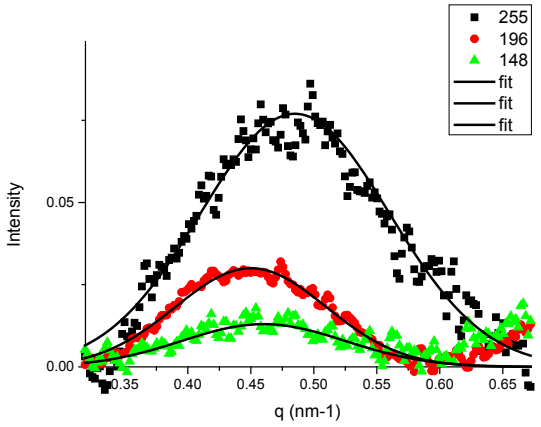

Figure S6. Rescaled SAXS spectra in the region around the radial peak for fibrin networks with varying fiber mass density, obtained by multiplying SAXS spectra with q^{Df} as in Figure 5 of the main text. Magnified view of a small region of the rescaled spectra after subtraction of the background level. Spectra are shown for networks with ρ = 255 mg/ml (black), 196 mg/ml (red) and 148 mg/ml (green). Solid black lines show Gaussian fits. From the FWHM, we estimate an average number of protofibrils per domain of $N_{avg}= 3\pm0.2$.